1521-0103/12/3412-493–499$25.00
THE JOURNAL OF PHARMACOLOGY AND EXPERIMENTAL THERAPEUTICS
Copyright © 2012 by The American Society for Pharmacology and Experimental Therapeutics
JPET 341:493–499, 2012
Vol. 341, No. 2
190660/3765518

Prevention of Bleomycin-Induced Lung Fibrosis in Mice by a Novel Approach of Parallel Inhibition of Cyclooxygenase and Nitric-Oxide Donation Using NCX 466, a Prototype Cyclooxygenase Inhibitor and Nitric-Oxide Donor

Alessandro Pini, Serena Viappiani, Manlio Bolla, Emanuela Masini, and Daniele Bani

Departments of Anatomy, Histology, and Forensic Medicine (A.P., D.B.) and Preclinical and Clinical Pharmacology (E.M.), University of Florence, Florence, Italy; and NicOx SA, Sophia-Antipolis, France (S.V., M.B.)

Received December 1, 2011; accepted February 13, 2012

ABSTRACT

Cyclooxygenase (COX)-inhibiting nitric oxide (NO) donors (CINODs) are designed to inhibit COX-1 and COX-2 while releasing NO. COX inhibition is responsible for anti-inflammatory and pain-relieving effects, whereas NO donation can improve microcirculation and exert anti-inflammatory and antioxidant actions. In an in vivo mouse model of bleomycin-induced lung fibrosis, we evaluated whether a prototype CINOD compound, (*S*)-(5*S*)-5,6-bis(nitrooxy)hexyl)2-(6-methoxynaphthalen-2-yl)propanoate (NCX 466), may show an advantage over naproxen, its congener drug not releasing NO. Bleomycin (0.05 IU) was instilled intratracheally to C57BL/6 mice, which were then treated orally with vehicle, NCX 466 (1.9 or 19 mg/kg), or an equimolar dose of naproxen (1 or 10 mg/kg) once daily for 14 days. Afterward, airway resistance, assumed as lung stiffness index, was assayed, and lung specimens were collected for analysis of lung inflammation and fibrosis. NCX 466 and naproxen dose-dependently prevented bleomycin-induced airway stiffness and collagen accumulation. NCX 466, at the highest dose, was significantly more effective than naproxen in reducing the levels of the profibrotic cytokine transforming growth factor-β and the oxidative stress markers thiobarbituric acid reactive substance and 8-hydroxy-2′-deoxyguanosine. NCX 466 also decreased myeloperoxidase activity, a leukocyte recruitment index, to a greater extent than naproxen. A similar inhibition of prostaglandin E_2 was achieved by both compounds. In conclusion, NCX 466 has shown a significantly higher efficacy than naproxen in reducing lung inflammation and preventing collagen accumulation. These findings suggest that COX inhibition along with NO donation may possess a therapeutic potential in lung inflammatory diseases with fibrotic outcome.

Introduction

Fibrosis can be considered an excessive reparative response of tissues to chronic injury and inflammation and is featured by excess deposition of collagen and other extracellular matrix components in the interstitium. Extracellular matrix accumulation disrupts the normal histologic architecture of an organ, eventually leading to its dysfunction (Kisseleva and Brenner, 2008; Paz and Shoenfeld, 2010). In spite of the diverse etiology and main target organs of fibrotic disorders, the common pathological hallmark is the presence of myofibroblasts, activated collagen-secreting fibroblasts, originated from stromal precursor cells that are induced to proliferate and differentiate by profibrotic factors released in the local inflammatory microenvironment, such as transforming growth factor-β (TGF-β) and angiotensin II (Wynn, 2007; Kisseleva and Brenner, 2008). In particular, fibrosis takes place when the synthesis of new collagen by myofibroblasts exceeds its degradation rate, leading to the accumulation of collagen over time (Wynn, 2008).

Pulmonary fibrosis is the end stage of a wide range of chronic lung inflammatory diseases, leading to progressive parenchymal destruction. Lung fibrosis is histopathologically characterized by alveolar and capillary loss caused by pneumocyte and endothelial apoptosis, excess interstitial collagen, accumulation of myofibroblasts, and abnormal remodeling of lung parenchyma (Hardie et al., 2009). This results in progressive airway stiffening and thickening of the air-blood

This work was supported by a grant from NicOx SA, Sophia-Antipolis, France (to D.B.).
Article, publication date, and citation information can be found at http://jpet.aspetjournals.org.
http://dx.doi.org/10.1124/jpet.111.190660.

ABBREVIATIONS: TGF-β, transforming growth factor-β; IPF, idiopathic pulmonary fibrosis; COX, cyclooxygenase; NO, nitric oxide; CINOD, COX-inhibiting NO donor; ROS, reactive oxygen species; MPO, myeloperoxidase; PAO, pressure at the airway opening; OD, optical density, 8-OHdG, 8-hydroxy-2′-deoxyguanosine; TBARS, thiobarbituric acid reactive substances; PGE_2, prostaglandin E_2; ANOVA, analysis of variance; ELISA, enzyme-linked immunosorbent assay; NCX 466, (*S*)-(5*S*)-5,6-bis(nitrooxy)hexyl)2-(6-methoxynaphthalen-2-yl)propanoate.

membrane, which makes breathing difficult and eventually leads to respiratory failure. Idiopathic pulmonary fibrosis (IPF), the most common and pernicious fibrotic disease of the lungs, has a particularly poor prognosis and represents a therapeutic challenge for pneumologists: in fact, the classic anti-inflammatory drugs have turned out to be nearly ineffective in improving its clinical course, being unable to prevent or delay the onset of respiratory failure. Therefore, the current therapeutic approaches to IPF are oriented toward novel substances that could override the limitations of the existing anti-inflammatory drugs, such as molecules targeting at the TGF-β signaling, the upstream activating pathway of myofibroblasts (Gharaee-Kermani et al., 2009). In this context, cyclooxygenase (COX) inhibiting nitric oxide (NO) donors (CINODs) are promising candidates, because they can add the donation of NO, a molecule known to improve microcirculation and exert anti-inflammatory and tissue-preserving effects via alternative pathways (Moncada et al., 1991), to the classic effects of prostaglandin inhibition. Of particular interest for lung fibrosis, NO has been described as possessing antifibrotic potential related to its ability to scavenge reactive oxygen species (ROS), such as peroxynitrite (Ferrer-Sueta and Radi, 2009) and reduce their local levels through enhanced microcirculatory dynamics. Cumulative evidence emerging from studies on the cirrhotic liver suggests that NO deficiency plays a major role in liver fibrosis and intrahepatic NO supplementation by NO donors may prevent liver cirrhosis by inhibiting the profibrotic activation of hepatic stellate cells induced by ROS or platelet-derived growth factor (Casini et al., 1997; Failli et al., 2000; Svegliati-Baroni et al., 2001). Moreover, circumstantial evidence in cultured rat mesangial cells, key mediators of glomerular inflammation and sclerosis, suggests that NO may have direct antifibrotic effects in kidney cells by down-regulating the expression of fibrosis-related genes (Wani et al., 2007).

Based on the above evidence, we decided to evaluate whether (*S*)-(5*S*)-5,6-bis(nitrooxy)hexyl)2-(6-methoxynaphthalen-2-yl)propanoate (NCX 466), a naproxen-based CINOD, would have therapeutic effects in an in vivo mouse model of bleomycin-induced lung fibrosis (Kaminski et al., 2000; Moeller et al., 2006). To support the rationale of this pharmacologic approach and evaluate the contribution of NO donation, NCX 466 has been compared in equimolar conditions with its congener naproxen, which does not release NO.

Materials and Methods

Drugs and Reagents. NCX 466 (molecular weight 436.42) was synthesized and provided by NicOx Research Institute (Bresso, Italy). Naproxen (molecular weight 230.3) was purchased from Sigma-Aldrich (Milan, Italy). NCX 466 and naproxen were suspended in a viscous vehicle (1% methylcellulose, 2% dimethyl sulfoxide, 5% Tween 80, and 5% castor oil) and administered by oral gavage. Unless otherwise stated, the reagents used were from Sigma-Aldrich.

Animals. Male C57BL/6 mice, approximately 2 months old and weighing 25 to 30 g, were used for the experiments. They were purchased from a commercial source (Harlan, Udine, Italy), fed a standard diet, and housed for at least 48 h under a 12-h light/dark photoperiod before the experiments. The study protocol complied with the Declaration of Helsinki and the recommendations of the European Economic Community (86/609/CEE) on animal experimentation and was approved by the ethical committee of the University of Florence, Florence, Italy. Experiments were carried out at the Centre for Laboratory Animal Housing and Experimentation, University of Florence.

Surgery and Treatments. Mice were anesthetized with zolazepam/tiletamine (Zoletil, Virbac Srl, Milan, Italy; 50 μg/g i.p. in 100 μl of saline); 35 of them were treated with bleomycin (0.05 IU in 100 μl of saline), and the other five were treated with 100 μl of saline (referred to as nonfibrotic negative controls), both delivered by tracheal puncture. Seven bleomycin-treated mice were given daily oral administrations of 100 μl of viscous vehicle: they are referred to as fibrotic positive controls. The remaining ones, seven per group, were given daily oral administrations of NCX 466 (1.9 or 19 mg/kg) or equimolar doses of naproxen (1 or 10 mg/kg) dissolved in 100 μl of viscous vehicle by an intragastric needle. The nonfibrotic negative control mice did not undergo further treatment. Oral administration of viscous vehicle, NCX 466, or naproxen was repeated at 9:00 AM on days 1 to 15 from surgery, with the exclusion of weekends, for a total of 10 daily doses. The noted oral doses of NCX 466 or naproxen were chosen by similarity with those found effective for inhibiting COX activity and preventing gastric damage in the rat (Muscará et al., 1998) and based on previous experiments in rodent models of inflammation. The range includes the EC_{50} for naproxen [e.g., in the carrageenan-induced paw edema in rat, NCX 466 and naproxen showed identical calculated ED_{50} (ED_{50} = 3.7 mg/kg)] (data not shown). In addition, inhibition of COX enzymes as measured by plasma thromboxane B_2 and PGE_2 was complete for the higher dose, but not for the lower dose (data not shown). The use of 1 and 10 mg/kg of naproxen in this in vivo model, and their equivalents for NCX 466, was therefore intended to explore a subeffective anti-inflammatory and a fully effective anti-inflammatory dose.

Functional Assay of Fibrosis. At day 14 after surgery, the mice were subjected to measurement of airway resistance to inflation, a functional parameter related to fibrosis-induced lung stiffness, by using a constant volume mechanical ventilation method (Masini et al., 2005). In brief, upon anesthesia, the mice were operated on to insert a 22-gauge cannula [Venflon 2 (Viggo Spectramed, Windlesham, UK), 0.8 mm diameter] into the trachea and then ventilated with a small-animal respirator (Ugo Basile, Comerio, Italy), adjusted to deliver a tidal volume of 0.8 ml at a rate of 20 strokes/min. Changes in lung resistance to inflation [pressure at the airway opening (PAO)] were registered by a high-sensitivity pressure transducer (P75 type 379; Harvard Apparatus Inc., Holliston, MA) connected to a polygraph (Harvard Apparatus Inc.; settings: gain 1, chart speed 25 mm/s). Inflation pressure was measured for at least 3 min. In each mouse, PAO measurements (expressed as millimeters) were carried out on at least 40 consecutive tracings of respiratory strokes and then averaged.

Lung Tissue Sampling. After the functional assay, the animals were killed, and the whole left lungs were excised and fixed by immersion in 4% formaldehyde in phosphate-buffered saline for histological analysis. The right lungs were weighed, quickly frozen, and stored at −80°C. When needed for the biochemical assays, these samples were thawed at 4°C, homogenized on ice in 50 mM Tris-HCl buffer containing 180 mM KCl and 10 mM EDTA, pH 7.4, and then centrifuged at 10,000*g*, 4°C, for 30 min, unless otherwise reported. The supernatants and the pellets were collected and used for separate assays as detailed below.

Histology and Computer-Aided Densitometry of Lung Collagen. Histological sections (6 μm thick) were cut from paraformaldehyde-fixed, paraffin-embedded lung samples and stained with hematoxylin and eosin for routine observation and with the modified Azan method for collagen fibers in which only aniline blue was used to reduce parenchymal tissue background. Staining was performed in a single session to minimize artifactual differences in collagen staining. In each mouse, 10 photomicrographs of peri-bronchial connective tissue were randomly taken by using a digital camera connected to a light microscope (Microstar IV; Reichert, Seefeld, Germany) with a 40× objective (test area of each micrograph: 38,700

μm^2). Measurements of optical density (OD) of the aniline blue-stained collagen fibers were carried out by using the ImageJ 1.33 image analysis program (http://rsb.info.nih.gov/ij), upon appropriate thresholding to exclude aerial air spaces and bronchial/alveolar epithelium as described previously (Formigli et al., 2007).

Determination of TGF-β. The levels of TGF-β, the major profibrotic cytokine involved in fibroblast activation (Wynn, 2008), were measured on aliquots (100 μl) of lung homogenate supernatants by using the Flow Cytomix assay (Bender Medsystems GmbH, Vienna, Austria), following the protocol provided by the manufacturer. In brief, a suspension of anti-TGF-β-coated beads was incubated with the samples (and a TGF-β standard curve) and then with biotin-conjugated secondary antibodies and streptavidin-phycoerythrin. Fluorescence was read with a cytofluorimeter (Epics XL; Beckman Coulter, Milan, Italy). Values are expressed as picogram/milligram of proteins, the latter determined with the Bradford method (Bradford, 1976) over an albumin standard curve.

Determination of Myeloperoxidase. This tissue indicator of leukocyte recruitment was determined on aliquots (100 μl) of lung homogenate supernatants, using a commercial ELISA kit (CardioMPO; Prognostix Inc., Cleveland, OH), according to the manufacturer's instructions. The values are expressed as milliunit/milligram of lung tissue (wet weight).

Determination of PGE_2. The levels of PGE_2, the major cyclooxygenase product generated by activated inflammatory cells, were measured on aliquots (100 μl) of lung homogenate supernatants by using commercial ELISA kits (Cayman Chemical, Ann Arbor, MI), following the protocol provided by the manufacturer. The values are expressed as nanogram/milligram of lung tissue (wet weight).

Determination of Thiobarbituric Acid-Reactive Substances. TBARS, such as malondialdehyde, are end-products of cell membrane lipid peroxidation by ROS and are considered reliable markers of oxidative tissue injury. They were determined by the measurement of the chromogen obtained from reaction of TBARS with 2-thiobarbituric acid (Aruoma et al., 1989). In brief, 0.5 ml of 2-thiobarbituric acid (1% w/v) in 50 mM NaOH and 0.5 ml of HCl (25% w/v in water) were added to the lung tissue pellets. The mixture was placed in test tubes, sealed with screw caps, and heated in boiling water for 10 min. After cooling, the chromogen was extracted in 3 ml of 1-butanol, and the organic phase was separated by centrifugation at 2000*g* for 10 min. The absorbance of the organic phase was read spectrophotometrically at 532-nm wavelength over a standard curve of 1,1,3,3-tetramethoxypropane. The values are expressed as nanomole/milligram of proteins, the latter determined with the Bradford method.

Determination of 8-Hydroxy-2′-Deoxyguanosine. Frozen lung samples were thawed at room temperature, and cell DNA isolation was performed as described previously (Lodovici et al., 2000) with minor modifications. The samples were homogenized in 1 ml of 10 mM phosphate-buffered saline, pH 7.4, sonicated on ice for 1 min, added to 1 ml of 10 mM Tris-HCl buffer, pH 8, containing 10 mM EDTA, 10 mM NaCl, and 0.5% SDS, and incubated for 1 h at 37°C with 20 μg/ml RNase. Samples were incubated overnight at 37°C in the presence of 100 μg/ml proteinase K. Afterward, the mixture was extracted with chloroform/isoamyl alcohol (10:2 v/v). DNA was precipitated from the aqueous phase with 0.2 volume of 10 M ammonium acetate, solubilized in 200 μl of 20 mM acetate buffer, pH 5.3, and denaturated at 90°C for 3 min. The extract was then supplemented with 10 IU of P1 nuclease in 10 μl and incubated for 1 h at 37°C with 5 IU of alkaline phosphatase in 0.4 M phosphate buffer, pH 8.8. All the procedures were performed in the dark. The mixture was filtered by an Amicon Micropure-EZ filter (Millipore Corporation, Billerica, MA), and 100 μl of each sample were used for 8OHdG determination by using an ELISA kit (JalCA, Shizuoka, Japan), following the instructions provided by the manufacturer. The values are expressed as nanogram/milligram of proteins, the latter determined by the Bradford method.

Statistical Analysis. For each assay, data were reported as mean values (± S.E.M.) of individual average measures of the different animals per group. Significance of differences among the groups was assessed by one-way ANOVA followed by Newman-Keuls post hoc test for multiple comparisons, using Prism 4.03 statistical software (GraphPad Software, Inc., San Diego, CA).

Results

Functional Assay of Fibrosis. Intratracheal bleomycin caused a statistically significant increase in airway stiffness, as judged by the clear-cut elevation of PAO in the fibrotic positive controls given oral vehicle (17.8 ± 0.6 mm) compared with the nonfibrotic negative controls (13.4 ± 0.6 mm). Both doses of NCX 466 (1.9 and 19 mg/kg) caused a statistically significant reduction of airway stiffness (14.0 ± 1.0 and 13.6 ± 0.6 mm, respectively). The results of the functional assay are shown in Fig. 1. The efficacy of NCX 466 seemed slightly higher than that of equimolar naproxen (15.3 ± 0.9 and 14.8 ± 1.0 mm at 1 and 10 mg/kg, respectively), although the differences did not reach statistical significance. For both drugs, the trend suggests a dose-dependent effect, although the differences between doses were not statistically significant.

Morphological and Morphometrical Analyses. Intratracheal bleomycin was found to cause lung inflammation and fibrosis. By conventional histology (Fig. 2), the lungs of the fibrotic positive controls given oral vehicle showed a marked inflammatory infiltrate in the peri-bronchial and interalveolar septa, which was absent in the nonfibrotic negative controls. The extent of the inflammatory infiltrate, which was composed mainly of macrophages, lymphocytes, and neutrophils, was reduced by both NCX 466 and naproxen at both tested doses. By computer-aided densitometry on Azan-stained sections (Fig. 3), which allows to determine the OD of collagen fibers, the lungs of the fibrotic positive controls showed a sharp, statistically significant increase in collagen fibers compared with the nonfibrotic negative controls. Administration of NCX 466 and naproxen at both doses caused a statistically significant reduction of the amount of lung collagen fibers. No statistical differences in collagen OD were observed between the high and low doses of either NCX 466 or naproxen or between equimolar NCX 466 and naproxen.

Determination of Inflammation and Fibrosis Parameters. Assay of TGF-β (Fig. 4), a major profibrotic cytokine, showed that this molecule increased significantly in the fibrotic positive controls given oral vehicle compared with the nonfibrotic negative controls. Administration of NCX 466 or naproxen caused statistically significant, dose-dependent reductions of TGF-β, NCX 466 being more effective than equimolar naproxen.

Determination of myeloperoxidase (MPO) (Fig. 5), an index of leukocyte accumulation into the inflamed lung tissue, showed that this parameter was markedly and significantly increased in the fibrotic positive controls compared with the nonfibrotic negative controls. Administration of NCX 466 and naproxen caused statistically significant, dose-dependent reductions of MPO. NCX 466 at both doses was significantly more effective than equimolar naproxen.

Determination of PGE_2 (Fig. 6), the major cyclooxygenase product generated by activated inflammatory cells, showed

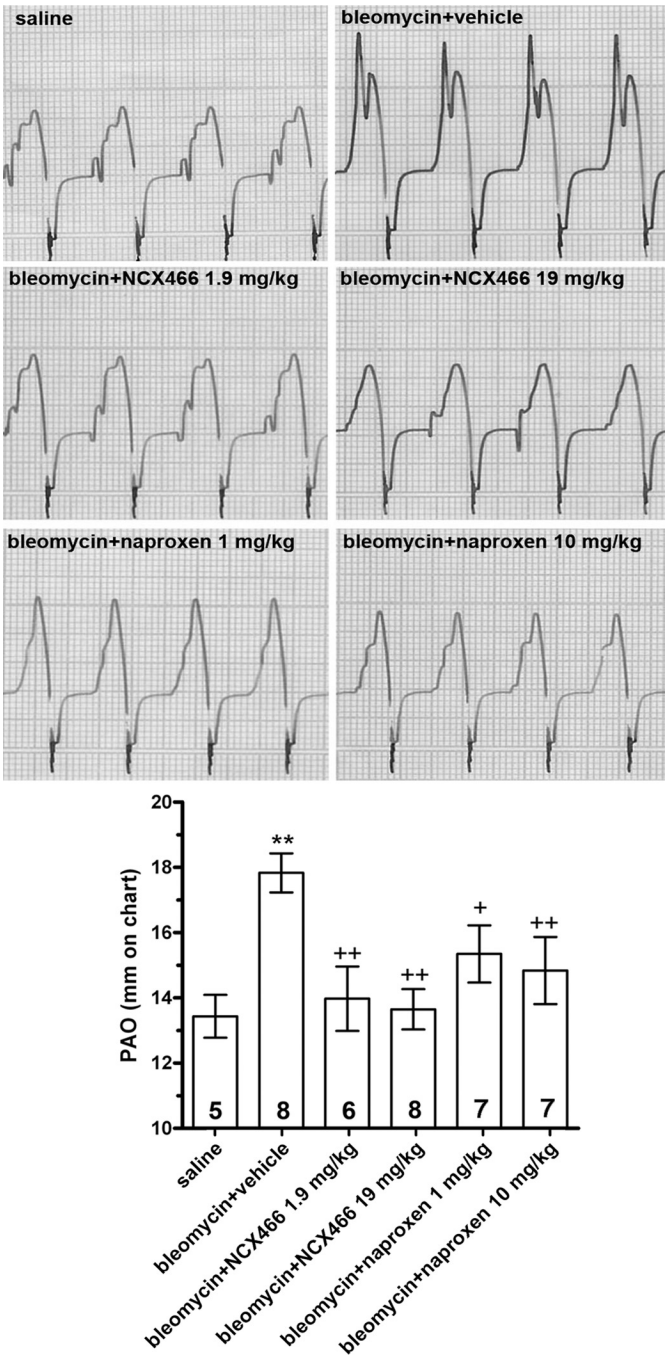

Fig. 1. Spirometric evaluation. Top, representative tracings of PAO measurements from mice of the different experimental groups. Bottom, bar graph and statistical analysis of differences of PAO values (means ± S.E.M.) between the different experimental groups (one-way ANOVA; n is indicated at the bottom of each bar). **, $p < 0.01$ versus saline. +, $p < 0.05$ and ++, $p < 0.01$ versus bleomycin + vehicle.

that this mediator was markedly increased in the fibrotic positive controls compared with the nonfibrotic negative controls. Administration of NCX 466 and naproxen caused a dose-dependent reduction of PGE_2 levels, which attained robust statistical significance at the higher dose, showing similar efficacy as equimolar naproxen.

Evaluation of Oxidative Stress Parameters. Measurement of TBARS (Fig. 7A), the end-products of cell membrane lipid peroxidation by ROS and reliable markers of oxidative

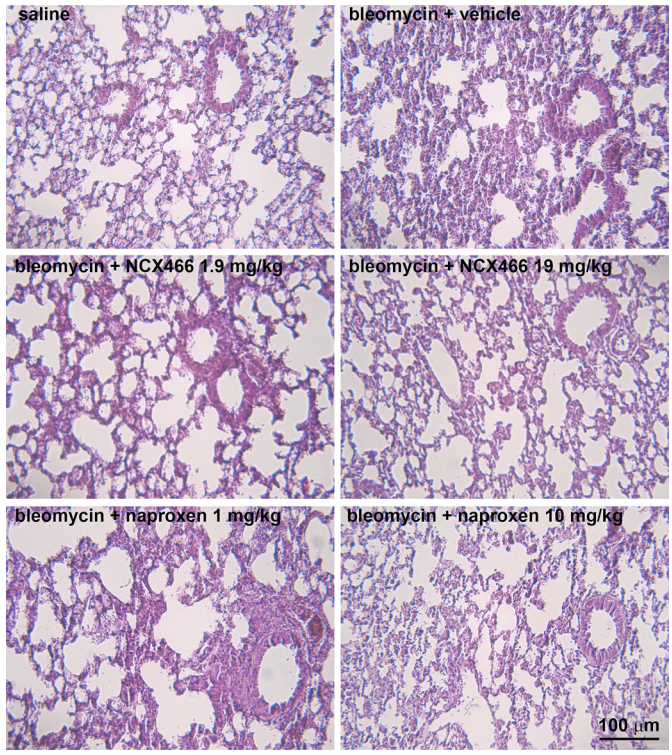

Fig. 2. Lung conventional histology. Representative micrographs of hematoxylin and eosin-stained lung tissue sections from mice of the different experimental groups. The lung from a fibrotic control given oral vehicle shows a prominent inflammatory infiltrate in the peri-bronchial and interalveolar septa, which was absent in the lung from a nonfibrotic negative control and was reduced by NCX 466 and naproxen at both of the tested doses.

tissue injury, showed that they were markedly increased in the fibrotic positive controls given oral vehicle compared with the nonfibrotic negative controls. Administration of NCX 466 and naproxen caused statistically significant, dose-dependent reductions of TBARS. NCX 466 at the higher dose was significantly more effective than equimolar naproxen. Determination of 8-OHdG (Fig. 7B), an indicator of oxidative DNA damage, showed a similar trend as TBARS, for it was markedly increased in the fibrotic positive controls compared with the nonfibrotic negative controls. Administration of NCX 466 and naproxen caused statistically significant, dose-dependent reductions of 8-OHdG. NCX 466 at both low and high doses was significantly more effective than equimolar naproxen.

Discussion

This study offers evidence that a CINOD compound can have therapeutic activity in a model of chemically induced lung fibrosis in the mouse. In our experiments, NCX 466 was administered orally in preventative mode, i.e., since the onset of bleomycin-induced lung injury, and has been compared with equimolar doses of naproxen. NCX 466 has shown sharp anti-inflammatory properties, for it consistently decreased the assayed histological and biochemical inflammatory parameters, i.e., the number of infiltrating leukocytes evaluated histologically, lung tissue MPO, and PGE_2 levels. When looking at the reduction of PGE_2 levels, which solely depend on COX inhibition, NCX 466 had similar efficacy as naproxen; on the other hand, when considering the other parameters, such as

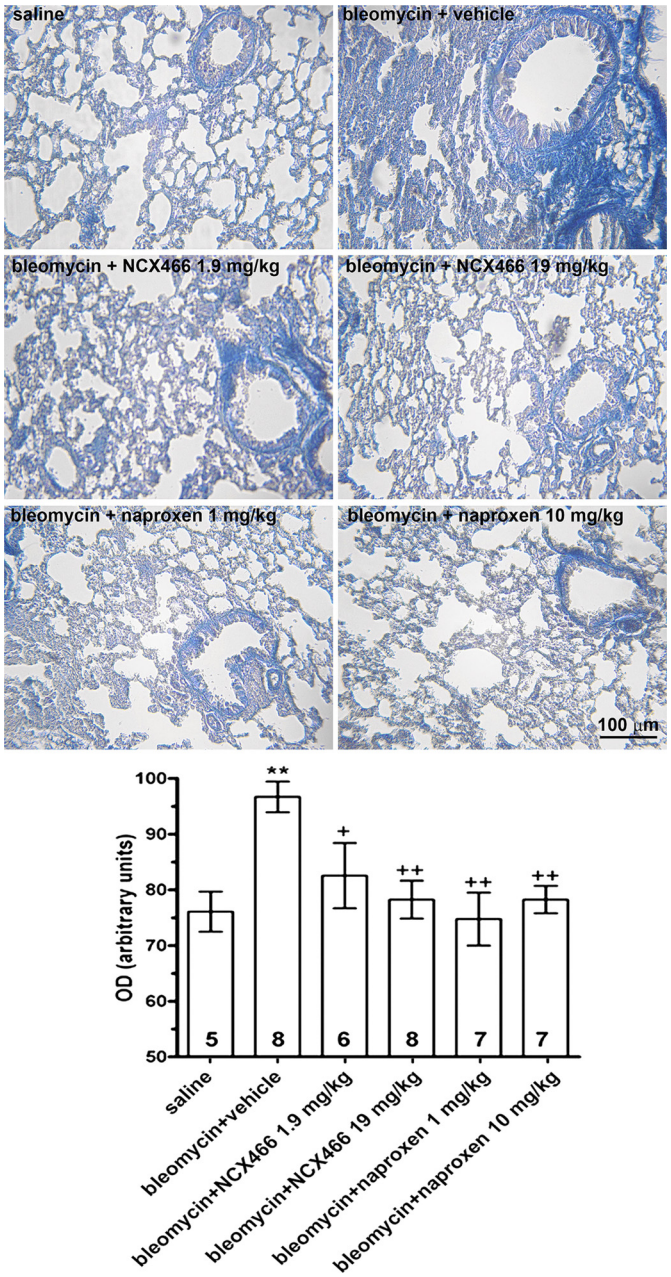

Fig. 3. Evaluation of lung fibrosis. Top, representative micrographs of Azan-stained lung tissue sections from mice of the different experimental groups. Collagen fibers are stained deep blue. The lung from a fibrotic control given oral vehicle shows marked fibrosis in the peri-bronchial stroma, which was absent in the lung from a nonfibrotic negative control and was reduced by NCX 466 and naproxen at both of the tested doses. Bottom, bar graph showing the OD (means ± S.E.M.) of Azan-stained collagen fibers of the different experimental groups (one-way ANOVA; n is indicated at the bottom of each bar). **, $p < 0.01$ versus saline. +, $p < 0.05$ and ++, $p < 0.01$ versus bleomycin + vehicle.

inhibition of leukocyte recruitment (histology and MPO) and oxidative stress (TBARS, 8-OHdG), NCX 466 was more effective than equimolar naproxen. This additional effect was conceivably caused by the NO released by NCX 466, which can have prominent effects on the vascular endothelium (Kubes et al., 1991; Laroux et al., 2000). NO can induce vasodilation, thereby increasing microcirculatory dynamics and local blood flow and favoring removal of proinflammatory mediators. These findings suggest a positive role of NO donation in the modulation of lung inflammatory pathways.

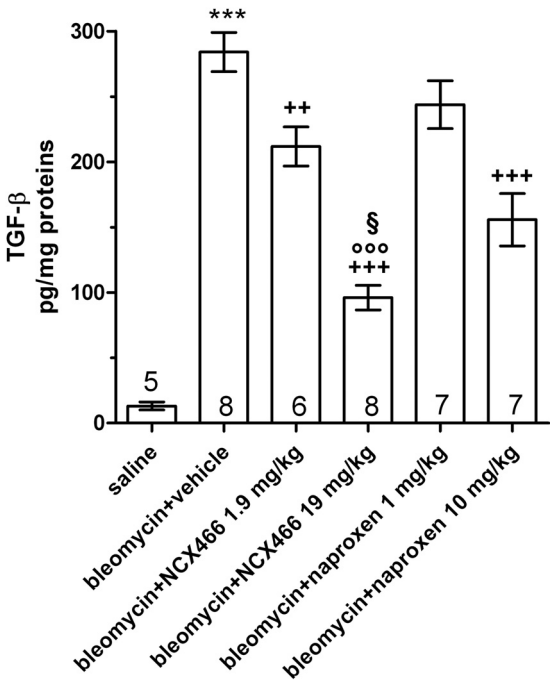

Fig. 4. Evaluation of TGF-β. Bar graph showing the lung tissue levels of the profibrotic cytokine (means ± S.E.M.) of the different experimental groups (one-way ANOVA; n is indicated at the bottom of each bar). ***, $p < 0.001$ versus saline. ++, $p < 0.01$ and +++, $p < 0.001$ versus bleomycin + vehicle. °°°, $p < 0.001$ versus NCX466 (1.9 mg/kg). §, $p < 0.05$ versus naproxen (10 mg/kg).

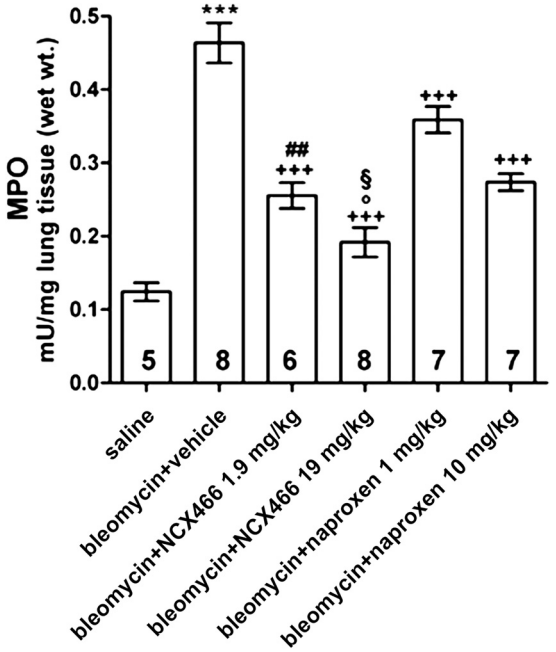

Fig. 5. Evaluation of leukocyte infiltration. Bar graph showing the lung tissue levels of MPO (means ± S.E.M.) of the different experimental groups (one-way ANOVA; n is indicated at the bottom of each bar). ***, $p < 0.001$ versus saline. +++, $p < 0.001$ versus bleomycin + vehicle. °, $p < 0.05$ versus NCX466 (1.9 mg/kg). ##, $p < 0.01$ versus naproxen (1 mg/kg). §, $p < 0.05$ versus naproxen (10 mg/kg).

It is noteworthy that NCX 466 caused a marked reduction of the lung levels of TGF-β, the major cytokine capable of shifting fibroblasts toward a fibrogenic phenotype (Wynn, 2008). This effect was already significant with the lower dose

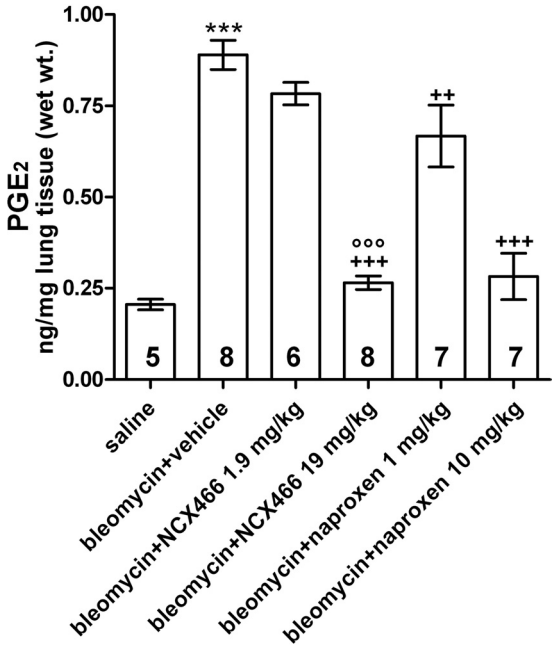

Fig. 6. Prostaglandin production. Bar graph showing the lung tissue levels of PGE_2 (means ± S.E.M.) of the different experimental groups (one-way ANOVA; n is indicated at the bottom of each bar). ***, $p < 0.001$ versus saline. ++, $p < 0.01$ and +++, $p < 0.001$ versus bleomycin + vehicle. °°°, $p < 0.001$ versus NCX 466 (1.9 mg/kg).

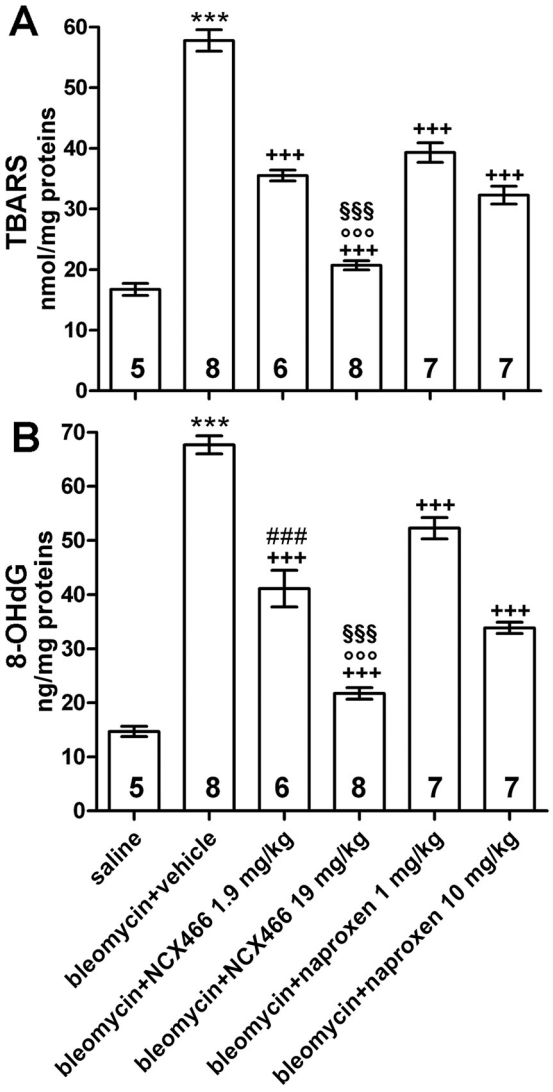

Fig. 7. Evaluation of oxidative stress parameters. Bar graphs showing the lung tissue levels of TBARS (A) and 8-OHdG (B) of the different experimental groups (one-way ANOVA; n is indicated at the bottom of each bar). ***, $p < 0.001$ versus saline. +++, $p < 0.001$ versus bleomycin + vehicle. °°°, $p < 0.001$ versus NCX466 (1.9 mg/kg). ###, $p < 0.001$ versus naproxen (1 mg/kg). §§§, $p < 0.001$ versus naproxen (10 mg/kg).

(1.9 mg/kg), whereas equimolar naproxen was almost ineffective. Accordingly, NCX 466 administration resulted in decreased lung fibrosis compared with the vehicle-treated positive controls, as shown by lung collagen morphometry. In turn, decreased airway stiffness can account for the reduction of PAO observed at the spirometric assay. With the used drug dosage and timing, we observed a slight advantage of NCX 466 over naproxen, although the measured differences were not significant. It is possible that with longer administration times this tendency may become more robust and reach statistical significance.

Pulmonary fibrosis, in particular IPF, represents a major human health hazard and cause of mortality, for which no antifibrotic therapy has shown a clear clinical efficacy (Wynn, 2007; Paz and Shoenfeld, 2010). Therefore, there is pressing demand for novel antifibrotic agents. Drugs targeting the TGF-β pathway, such as anti-TGF-β monoclonal antibodies and the fibroblast inhibitor pirfenidone, hold great promise and are subjects of recent clinical trials (Prud'homme, 2007). Although the preliminary data seem encouraging, their therapeutic efficacy on patients with IPF still remains to be clearly demonstrated (Paz and Shoenfeld, 2010). On the other hand, the strategy of targeting prostaglandin synthesis by classic nonsteroidal anti-inflammatory drugs is questioned by controversial findings. Although COX inhibitors, such as indomethacin, diclofenac, and meloxicam, were reported to prevent or reduce lung collagen accumulation, inflammation, and oxidative stress in bleomycin-induced lung fibrosis models (Thrall et al., 1979; Chandler and Young, 1989; Arafa et al., 2007), evidence also exists that PGE_2 inhibits fibroblast proliferation and collagen production (Saltzman et al., 1982) and patients with pulmonary fibrosis have decreased PGE_2 levels and may benefit from aerosolic PGE_2 administration (Borok et al., 1991). In keeping with this notion, COX-2-deficient mice showed an enhanced fibrogenic response to bleomycin (Keerthisingam et al., 2001), and the administration of indomethacin to mice during the fibrogenic phase postbleomycin worsened the severity of fibrosis (Moore et al., 2000). These data suggest an ambiguous role of PGE_2 in lung fibroblast homeostasis and the evolution of lung fibrotic lesions. It is conceivable that prostaglandin inhibition may have favorable effects on pulmonary fibrosis during the overt inflammatory phase of the disease and detrimental effects during the postinflammatory fibrogenic phase. In this context, the present study points at NCX 466 as a promising candidate drug for pulmonary fibrosis because of its NO-releasing properties. In fact, established IPF lacks an overt inflammatory component and rather seems as a dysregulation of the fibrogenic behavior of lung fibroblasts (Selman et al., 2001; Hardie et al., 2009). On these cells, NO released by NCX 466 could play a down-regulatory role, as shown by numerous in vivo and in vitro models of fibrosis (Casini et al., 1997; Failli et al., 2000; Svegliati-Baroni et al.,

2001; Wani et al., 2007; Ferrer-Sueta and Radi, 2009). Moreover, patients suffering for chronic fibrotic diseases need to take medications for a long time, exposing them to an increased risk for adverse side effects. The advantages of CINODs over the classic nonsteroidal anti-inflammatory drugs, namely similar or improved pharmacokinetic and efficacy profiles (Fagerholm and Björnsson, 2005; Hill et al., 2006) accompanied by better blood pressure control (White et al., 2009) and gastro-duodenal safety (Wilder-Smith et al., 2006), may become relevant for the setup of long-term therapeutic protocols. Because of their obvious clinical implications, CINODs deserve further investigation, e.g., using transgenic animals transiently expressing profibrotic genes that may reproduce the pathogenic events of IPF (Moeller et al., 2006).

Acknowledgments

We thank Laura Calosi (Department of Anatomy, Histology, and Forensic Medicine, University of Florence, Florence, Italy) for skilful technical support in histology.

Authorship Contributions

Participated in research design: Viappiani, Bolla, and Bani.
Conducted experiments: Pini, Masini, and Bani.
*Performed data analysis:*Pini, Masini, and Bani.
Wrote or contributed to the writing of the manuscript: Pini, Viappiani, Bolla, and Bani.

References

Arafa HM, Abdel-Wahab MH, El-Shafeey MF, Badary OA, and Hamada FM (2007) Anti-fibrotic effect of meloxicam in a murine lung fibrosis model. *Eur J Pharmacol* **564:**181–189.
Aruoma OI, Halliwell B, Laughton MJ, Quinlan GJ, and Gutteridge JM (1989) The mechanism of initiation of lipid peroxidation: evidence against a requirement for an iron (II)-iron (III) complex. *Biochem J* **258:**617–620.
Borok Z, Gillissen A, Buhl R, Hoyt RF, Hubbard RC, Ozaki T, Rennard SI, and Crystal RG (1991) Augmentation of functional prostaglandin E levels on the respiratory epithelial surface by aerosol administration of prostaglandin E. *Am Rev Respir Dis* **144:**1080–1084.
Bradford MM (1976) A rapid and sensitive method for the quantitation of microgram quantities of protein utilizing the principle of protein-dye binding. *Anal Biochem* **72:**248–254.
Casini A, Ceni E, Salzano R, Biondi P, Parola M, Galli A, Foschi M, Caligiuri A, Pinzani M, and Surrenti C (1997) Neutrophil-derived superoxide anion induces lipid peroxidation and stimulates collagen synthesis in human hepatic stellate cells: role of nitric oxide. *Hepatology* **25:**361–367.
Chandler DB and Young K (1989) The effect of diclofenac acid (Voltaren) on bleomycin-induced pulmonary fibrosis in hamsters. *Prostaglandins Leukot Essent Fatty Acids* **38:**9–14.
Fagerholm U and Björnsson MA (2005) Clinical pharmacokinetics of the cyclooxygenase inhibiting nitric oxide donator (CINOD) AZD3582. *J Pharm Pharmacol* **57:**1539–1554.
Failli P, DeFranco RM, Caligiuri A, Gentilini A, Romanelli RG, Marra F, Batignani G, Guerra CT, Laffi G, Gentilini P, et al. (2000) Nitrovasodilators inhibit platelet-derived growth factor-induced proliferation and migration of activated human hepatic stellate cells. *Gastroenterology* **119:**479–492.
Ferrer-Sueta G and Radi R (2009) Chemical biology of peroxynitrite: kinetics, diffusion, and radicals. *ACS Chem Biol* **4:**161–177.
Formigli L, Perna AM, Meacci E, Cinci L, Margheri M, Nistri S, Tani A, Silvertown J, Orlandini G, Porciani C, et al. (2007) Paracrine effects of transplanted myoblasts and relaxin on post-infarction heart remodeling. *J Cell Mol Med* **11:**1087–1110.
Gharaee-Kermani M, Hu B, Phan SH, and Gyetko MR (2009) Recent advances in molecular targets and treatment of idiopathic pulmonary fibrosis: focus on TGFβ signaling and the myofibroblast. *Curr Med Chem* **16:**1400–1417.
Hardie WD, Glasser SW, and Hagood JS (2009) Emerging concepts in the pathogenesis of lung fibrosis. *Am J Pathol* **175:**3–16.
Hill CM, Sindet-Pederson S, Seymour RA, Hawkesford JE 2nd, Coulthard P, Lamey PJ, Cowan CG, Wickens M, Jeppsson L, Dean AD, et al. (2006) Analgesic efficacy of the cyclooxygenase-inhibiting nitric oxide donor AZD3582 in postoperative dental pain: comparison with naproxen and rofecoxib in two randomized, double-blind, placebo-controlled studies. *Clin Ther* **28:**1279–1295.
Kaminski N, Allard JD, Pittet JF, Zuo F, Griffiths MJ, Morris D, Huang X, Sheppard D, and Heller RA (2000) Global analysis of gene expression in pulmonary fibrosis reveals distinct programs regulating lung inflammation and fibrosis. *Proc Natl Acad Sci U S A* **97:**1778–1783.
Keerthisingam CB, Jenkins RG, Harrison NK, Hernandez-Rodriguez NA, Booth H, Laurent GJ, Hart SL, Foster ML, and McAnulty RJ (2001) Cyclooxygenase-2 deficiency results in a loss of the anti-proliferative response to transforming growth factor-β in human fibrotic lung fibroblasts and promotes bleomycin-induced pulmonary fibrosis in mice. *Am J Pathol* **158:**1411–1422.
Kisseleva T and Brenner DA (2008) Mechanisms of fibrogenesis. *Exp Biol Med (Maywood)* **233:**109–122.
Kubes P, Suzuki M, and Granger DN (1991) Nitric oxide: an endogenous modulator of leukocyte adhesion. *Proc Natl Acad Sci U S A* **88:**4651–4655.
Laroux FS, Lefer DJ, Kawachi S, Scalia R, Cockrell AS, Gray L, Van der Heyde H, Hoffman JM, and Grisham MB (2000) Role of nitric oxide in the regulation of acute and chronic inflammation. *Antioxid Redox Signal* **2:**391–396.
Lodovici M, Casalini C, Cariaggi R, Michelucci L, and Dolara P (2000) Levels of 8-hydroxydeoxyguanosine as a marker of DNA damage in human leukocytes. *Free Radic Biol Med* **28:**13–17.
Masini E, Bani D, Vannacci A, Pierpaoli S, Mannaioni PF, Comhair SA, Xu W, Muscoli C, Erzurum SC, and Salvemini D (2005) Reduction of antigen-induced respiratory abnormalities and airway inflammation in sensitized guinea pigs by a superoxide dismutase mimetic. *Free Radic Biol Med* **39:**520–531.
Moeller A, Rodriguez-Lecompte JC, Wang L, Gauldie J, and Kolb M (2006) Models of pulmonary fibrosis. *Drug Discov Today Dis Models* **3:**243–249.
Moncada S, Palmer RM, and Higgs EA (1991) Nitric oxide: physiology, pathophysiology, and pharmacology. *Pharmacol Rev* **43:**109–142.
Moore BB, Coffey MJ, Christensen P, Sitterding S, Ngan R, Wilke CA, McDonald R, Phare SM, Peters-Golden M, Paine R 3rd, et al. (2000) GM-CSF regulates bleomycin-induced pulmonary fibrosis via a prostaglandin-dependent mechanism. *J Immunol* **165:**4032–4039.
Muscará MN, McKnight W, Del Soldato P, and Wallace JL (1998) Effect of a nitric oxide-releasing naproxen derivative on hypertension and gastric damage induced by chronic nitric oxide inhibition in the rat. *Life Sci* **62:**PL235–PL240.
Paz Z and Shoenfeld Y (2010) Antifibrosis: to reverse the irreversible. *Clin Rev Allergy Immunol* **38:**276–286.
Prud'homme GJ (2007) Pathobiology of transforming growth factor in cancer, fibrosis and immunologic disease, and therapeutic considerations. *Lab Invest* **87:**1077–1091.
Saltzman LE, Moss J, Berg RA, Hom B, and Crystal RG (1982) Modulation of collagen production by fibroblasts. Effects of chronic exposure to agonists that increase intracellular cyclic AMP. *Biochem J* **204:**25–30.
Selman M, King TE, Pardo A, American Thoracic Society, European Respiratory Society, and American College of Chest Physicians (2001) Idiopathic pulmonary fibrosis: prevailing and evolving hypotheses about its pathogenesis and implications for therapy. *Ann Intern Med* **134:**136–151.
Svegliati-Baroni G, Saccomanno S, van Goor H, Jansen P, Benedetti A, and Moshage H (2001) Involvement of reactive oxygen species and nitric oxide radicals in activation and proliferation of rat hepatic stellate cells. *Liver* **21:**1–12.
Thrall RS, McCormick JR, Jack RM, McReynolds RA, and Ward PA (1979) Bleomycin-induced pulmonary fibrosis in the rat: inhibition by indomethacin. *Am J Pathol* **95:**117–130.
Wani J, Carl M, Henger A, Nelson PJ, and Rupprecht H (2007) Nitric oxide modulates expression of extracellular matrix genes linked to fibrosis in kidney mesangial cells. *Biol Chem* **388:**497–506.
White WB, Schnitzer TJ, Fleming R, Duquesroix B, and Beekman M (2009) Effects of the cyclooxygenase inhibiting nitric oxide donator naproxcinod versus naproxen on systemic blood pressure in patients with osteoarthritis. *Am J Cardiol* **104:**840–845.
Wilder-Smith CH, Jonzon B, Fornstedt-Wallin B, Hedman A, and Karlsson P (2006) Dose-effect comparisons of the CINOD AZD3582 and naproxen on upper gastrointestinal tract mucosal injury in healthy subjects. *Scand J Gastroenterol* **41:**264–273.
Wynn TA (2007) Common and unique mechanisms regulate fibrosis in various fibroproliferative diseases. *J Clin Invest* **117:**524–529.
Wynn TA (2008) Cellular and molecular mechanisms of fibrosis. *J Pathol* **214:**199–210.

Address correspondence to: Dr. Daniele Bani, Department of Anatomy, Histology, and Forensic Medicine, Section of Histology, University of Florence, viale G. Pieraccini 6, I-50139 Florence, Italy. E-mail: daniele.bani@unifi.it